Radiation belt electron acceleration by ULF wave drift resonance: Simulation of 1997 and 1998 storms

Mary K. Hudson, Scot R. Elkington, John G. Lyon, M. Wiltberger and Marc Lessard[1]

Short title: RADIATION BELT ELECTRON ACCELERATION BY ULF WAVES

[1]Dartmouth College, Hanover, New Hampshire

Abstract.

Pc 5 ULF waves are seen concurrently with the rise in radiation belt fluxes associated with CME-magnetic cloud events. Four such geomagnetic storm periods in 1997 and 1998, 10-11 January and 14-15 May, 1997; 1-4 May and 26-28 August, 1998, have been simulated with a 3D global MHD code driven by L1-measured solar wind parameters. The field output has been used to advance electron guiding center trajectories in the equatorial plane. The time series has also been analyzed for ULF wave mode structure. Toroidal field line resonances with low azimuthal mode number and frequencies commensurate with the electron drift period are identified in the radial electric field component, along with enhanced power in the poloidal (azimuthal) electric field component. The simulated time scale for inward radial transport of electrons in the several hundred keV to MeV energy range, from geosynchronous orbit to L=3-4, varies with the level of ULF wave power and overall energy input to the magnetosphere. Of the four events studied, the May 1998 storm period was most geoeffective and the January 1997 least so, in terms of simulated radial transport and energization of electrons. This transport rate is consistent with the level of ULF waves excited in the simulations, and the proposed drift resonant acceleration mechanism.

INTRODUCTION

ULF waves have recently been shown to correlate well with relativistic electron flux enhancements, both during recurring high speed stream periods at solar minimum (Rostoker et al., 1998) and for CME-driven storm periods approaching solar maximum (Baker et al., 1998a; 1998b; Hudson et al., 1999). This paper presents analysis of four recent stormtime simulations in 1997 and 1998, initiated by a CME-driven change in solar wind input to the magnetosphere. Parameters measured at the WIND spacecraft have been used to drive a 3D global MHD simulation (Goodrich et al., 1998) for the four storms. The field output from these simulations has been analyzed for MHD mode structure (Hudson et al., 2000), and used as input to a guiding center test particle code which advances electron flux in the equatorial plane (Hudson et al., 1999). This paper compares the relative geoeffectiveness of the four storms, as measured by the rate of relativistic electron radial transport and first invariant conserving acceleration. The January 1997 storm had a moderate Dst response (~ -78 nT), and was characterized by a relatively low solar wind speed of 400-450 km/s, increasing to 400-500 km/s for the May 1997 storm (Dst ~ -115 nT), and almost double (850 km/s at maximum) its nominal value for the May and August 1998 events (Dst ~-216 and -188 nT, respectively). Although the January 1997 storm was noteworthy for the high density (180 cm^3) solar wind impulse early on 11 January, during the northward IMF B_z period of this magnetic cloud passage (Burlaga et al., 1998), the greatest relativistic electron flux increase occurred during the preceeding southward IMF B_z period (Reeves et al., 1998a; 1998b). A growing body of evidence suggests that the solar wind speed (Paulikas and Blake, 1979), in combination with southward IMF B_z (Blake et al., 1997), is the main factor in producing relativistic electron flux enhancement in the magnetosphere. This paper focuses on analysis of the role ULF waves play in mediating the transfer of energy from the solar wind to the electrons.

The time scale for acceleration seen in the four simulation studies, a period of hours to a day, is intermediate between the time scale of days for standard radial diffusion models, confirmed for a relatively quiet period in 1996 using Polar measurements (Selesnick and Blake, 1997), and very rapid injection on an electron drift time scale, as seen for the extreme CME-shock event of March 24, 1991 (Blake et al., 1992; Li et al., 1993), where the interplanetary shock speed was estimated to be as high as 1400 km/s (Shea and Smart, 1993). Both an analytic model (Li et al., 1993; Hudson et al., 1995) and MHD simulation (Hudson et al., 1996; Hudson et al., 1997) have been used to characterize acceleration by the azimuthal electric field associated with this extreme SSC compression of the magnetosphere. An impulsive azimuthal electric field in excess of 100 mV/m was estimated for the dayside outer magnetosphere based on measured fields of 20 mV/m on the nightside within the plasmaphere (Wygant et al., 1994). The SSCs of the four storms simulated here were moderate by comparison.

SIMULATIONS

Figure 1 shows a sequential comparison of the electron integral flux vs. energy and L for the four storms, using an AE8MIN input spectrum (Vette, 1991). Electron guiding center trajectories were advanced in the equatorial plane using field output from the Lyon-Fedder-Mobarry 3D global MHD code for the respective storms (Goodrich et al., 1998). Fields are interpolated from the MHD grid to the location of particle guiding centers and a test on first invariant conservation, well maintained for electrons, is imposed. One sees the most rapid inward radial transport and energization, given by first invariant conservation, for the May 1998 storm (7.5 hours shown), and longest time scale for the January 1997 storm (14.5 hours shown). Inner zone flux changes are not followed because of the L=2.3 inner boundary of the MHD simulation. Outer zone fluxes are transported radialy inward to fill the slot region for all four storm comparisons.

While the May 1998 event shows the most rapid radial transport, several factors make this event difficult to compare directly with particle observations, in particular the fact that the 4 May storm occurred during the recovery phase of one initiated on 2 May. Comparing the use of AE8MIN or AE8MAX as a source population was found to make only a small difference in final results. However, initiating the simulation with an input differential flux spectrum normalized to measurements from a HEO spacecraft, with 55 degree inclination in a geosynchronous-transfer orbit, shows significant variation from the AE8 model for the May 1998 event (Figure 2). Using the HEO spectrum measured on 1 May to initialize the simulation, before any significant storm disturbance, yields a peak electron flux reduced at energies above 2 MeV (compare with Figure 1b), a result which is consistent with observations from the SAMPEX and POLAR satellites (Selesnick et al., 2000; Blake et al., 1998). This comparison shows model sensitivity to the assumed source population.

Analysis of the azimuthal mode number at a fixed radial location in each field component, indicates that power is concentrated at $m < 5$ (Elkington, 2000), also seen in snapshots of electric field vectors in the equatorial plane (Hudson et al., 1999; 2000). An FFT analysis of 2-3 hour time intervals of the radial and azimuthal electric field components at a fixed longitude determines the frequency spectrum. Figure 3 shows the power spectrum of the radial electric field component at midnight LT for 26 and 27 August 1998, produced for two three-hour intervals. The same toroidal field line resonant mode structure is evident in the radial electric field component as was seen in simulating the 10-11 January 1997 event (Hudson et al., 1999; 2000). A comparison is made in Figure 3 of the radial power profile following arrival of the interplanetary shock at 0640 UT on 26 August, during a period of IMF $B_z > 0$, with increased power at higher frequencies and lower L values during the $\sim$ 24 hour period of IMF $B_z < 0$ on 27 August. Straight lines plotted indicate electron drift frequency at a specified energy and L value, with positive slope corresponding to constant energy vs. L and negative slope corresponding to constant first invariant. The simulated ULF wave power in the radial and the azimuthal (not shown) electric field component is greater during the negative B_z

interval on 27 August than following the interplanetary shock arrival on 26 August. This result, which is found consistently for all four storms, is confirmed by spectral analysis of GOES magnetometer data in mean field coordinates, plotted in Figure 4 for the August 1998 event. The middle panel shows the azimuthal magnetic field component while the top and bottom panels show the radial and compressional components. No direct comparison can be made between the two 24 hour intervals covering all local times in Figure 4 and the fixed local time analysis of Figure 3, except to note the greater ULF wave activity and power on 27 August during southward IMF B_z. This dependence of ULF wave power on IMF B_z was seen in the GOES magnetetometer data for all four storms (http://engineering.dartmouth.edu/ spacescience/storms/goes_plots.html).

DISCUSSION

The MHD-test particle simulations confirm the observed correlation between ULF oscillations and inward radial transport and energization of relativistic electrons. The time scale of the transport is consistent with the drift resonant acceleration process proposed by Hudson et al. (1999; 2000) and analyzed in detail by Elkington et al. (1999), who followed a smaller number of test particles in a simplified field model. Acceleration via drift resonance with the radial electric field component comes about because of the non-axisymmetric drift path (Hudson et al., 1999; 2000). An electron with drift frequency $\omega_D = \omega$, the toroidal mode wave frequency, sees a radial electric field oscillating in phase with its drift period, which can lead to continuous acceleration via radial motion in a non-axisymmetric dipole. A similar effect is obtained for the poloidal mode with oscillatory azimuthal electric field in a non-axisymmetric dipole (Elkington, 2000). Resonance with a spectrum of ULF wave frequencies and azimuthal mode numbers is possible, with multiple resonances of finite width in energy and L evident in Figure 3.

To simplify the analysis, Elkington et al. (1999) assumed a tailward displaced dipole magnetic field and a superposed electric field including a uniform dawn-dusk convection field and a summation over m of sinousoidal radial and azimuthal oscilatory components, to simulate poloidal and toroidal modes:

$$B(r, \phi) = \frac{B_0}{r^3} + b_1(1 + b_2 \cos\phi). \tag{1}$$

$$E(r, \phi, t) = E_0(r, \phi) + \sum_{m=0}^{\infty} \delta E_{rm} \sin(m\phi + \omega t + \xi_m) \tag{2}$$

The longest wavelength toroidal mode has a null in oscilatory B_ϕ in the equatorial plane, and maximum E_r, while the corresponding poloidal mode has a null in B_r and maximum in both E_ϕ and compressional B_z components (Cummings et al., 1969). The latter can be neglected at low beta (ratio of kinetic to magnetic pressure) for low azimuthal mode numbers. Bulk energization of an ensemble of 120 particles distributed in drift phase was obtained with a single toroidal mode with frequency corresponding to the initial electron drift frequency. For a range of initial electron energies (40 keV to 5 MeV), resonances corresponding to $(m \pm 1)\omega_D = \omega$ produced energization.

Figure 3 shows the presence of multiple field line resonant frequencies at a given L value. Overlapping resonances result in a continuem of accessable energy-drift phase space, leading to a calculable diffusion time scale of hours to a day (Elkington, 2000), depending on wave power. Poloidal modes (azimuthal electric field perturbation) contribute a comparable amount of acceleration; the non-axisymmetric dipole increases efficiency over standard radial diffusion calculations (Falthammar, 1968). Elkington's calculation assumes wave power consistent with that seen in Figure 3, leading to radial transport and first invariant-conserving energization scaling as $L^{-3/2}$ for relativistic electrons. The convection electric field, which is self-consistently included in the MHD simulation, is also enhanced during periods of increased solar wind coupling. Including a simplified, uniform dawn-dusk E_0 in the model calculation increases the radial distortion of the drift orbit, hence rate of radial transport and energization (Elkington et al., 1999).

Direct comparison with measured electron flux requires careful consideration of the input source population, spacecraft location and detector response (Li et al., 1998; 1999). Increase in the magnitude of D_{st} causes a measurable dropout in geosynchronous electron flux in all four events, due to main phase buildup of the ring current and third invariant conservation (Kim and Chan, 1998). Plots of relative energy flux in four energy channels measured by GPS spacecraft at their equatorial radial crossing point have reproduced the decrease in flux associated with D_{st} (Hudson et al., 1999); for simulated geosynchronous orbit, magnetosheath encounters that coincide with those seen by LANL spacecraft are also reproduced by the MHD-test particle simulations (Hudson et al., 2000), as is the diurnal variation in geosynchronous flux due to the compressed dipole, enhanced during storm periods (Elkington, 2000).

CONCLUSIONS

A comparison of MHD-test particle simulations of four geomagnetic storms driven by CME-generated perturbations of the solar wind has been presented. All four storms were characterized by a buildup of relativistic electron flux in the inner magnetosphere (see ISTP and GEM web sites). The fastest inward radial transport and energization is seen in simulating the May 1998 event, using the AE8MIN initial flux profile for all four storms. The flux above 2 MeV is reduced when an input profile measured by a HEO spacecraft on 1 May 1998 is used. However, this input profile preceeds the geomagnetic storm on 2 May, and is shown simply to demonstrate effects of varying the source population. The ULF wave power was also greatest for the May 1998 storm. This event proves to be the most complex of the four to analyze because of the highly compressed state of the magnetosphere (magnetopause compressed into L=4 around 0300 UT on 4 May). We will not attempt a direct comparison with measured particle flux changes, except to note that the range from 12 hours for rise in flux of $>$ 2 MeV electrons at L=4 on 10 January 1997 (Reeves et al., 1998a) to 3 hours as an upper limit on the time scale for 600-700 keV electrons to fill the slot region on 4 May 1998 (Blake et al., 1998) is consistent with acceleration rates seen in the simulations of these events, at the extremes of the four studied. The absence of slot region filling at energies > 2 MeV for the May 1998 event (Blake et al., 1998) is consistent with rapid loss to the magnetopause of electrons at L > 4, which would have acquired more energy via radial transport than those initially inside L=4 (Li et al., 1993).

The time scale for accleration is hours to roughly a day for all four storms. The stronger the solar wind driver, or solar wind speed as well as prolonged southward IMF B_z, the faster the radial transport and corresponding first-invariant conserving acceleration. Enhanced ULF wave power has the same toroidal mode structure for both the January 1997 and August 1998 simulations, even though solar wind driving conditions were substantially different. There is more simulated power extending to higher frequencies for the May 1998 event (not shown), least for January 1997 (Hudson et al., 1999; 2000), and a comparable amount for May 1997 as for August 1998 (Figure 3). These results are born out in analysis of GOES magnetometer data for the four events.

The global MHD simulations provide an opportunity for ULF wave mode structure analysis not possible with a limited set of spacecraft. Using MHD output fields to advance electron guiding center trajectories provides insight into relative transport rates for different storms. However, the technique is still in its infancy in terms of source population, with work in progress to provide data assmilation (Moorer and Baker, 2000) which would improve upon AE8 or CRRES-based average models (Brautigam and Albert, 2000) as a starting point.

Acknowledgments. We thank J. F. Fennell for providing HEO data, J. B. Blake for discussions of Polar, HEO and Sampex data, and A. A. Chan for discussion and analysis of the acceleration mechanism. This work is supported by NASA grants NAG5-7442, NAG5-8441 and NAG5-7689 to Dartmouth College, along with NSF grant ATM9819927.

References

Brautigam, D.H and J.M. Albert, Radial diffusion analysis of outer radiation belt electrons during the October 9, 1990, magnetic storm, *J. Geophys. Res., 105*, 291, 2000.

Baker, D. N., T. I. Pulkkinen, X. Li, S. G. Kanekal, J. B. Blake, R. S. Selesnick, M. G. Henderson, G. D. Reeves, H. E. Spence and G. Rostoker, Coronal mass ejections, magnetic clouds, and relativistic magnetospheric electron events: ISTP, *J. Geophys. Res., 103,* 17279, 1998a.

Baker, D. N., T. I. Pulkkinen, X. Li, S. G. Kanekal, K. W. Ogilvie, R. P. Lepping, J. B. Blake, L. B. Callis, G. Rostoker, H. J. Singer and G. D. Reeves, A strong CME-related magnetic cloud interaction with the Earth's magnetosphere: ISTP observations of rapid relativistic electron acceleration on May 15, 1997, *Geophys. Res. Lett., 25,*2975, 1998b.

Blake, J. B., W. A. Kolasinski, R. W. Filius and E. G. Mullen, Injection of electrons and protons with energies of tens of MeV into L , 3 on March 24, 1991, *Geophys. Res. Lett., 19*, 821, 1992.

Blake, J. B., D. N. Baker, N. Turner, K. W. Ogilvie, and R. P. Lepping, Correlation of changes in the outer-zone relativistic-electron population with upstream solar wind and magnetic field measurements, *Geophys. Res. Lett., 24,* 927, 1997.

Blake, J. B., M. D. Looper, J. E. Mazur, D. N. Baker, X. Li, M. K. Hudson, S. G. Kanekal, R. A. Mewaldt, Multi-satellite observations of the injection of energetic radiation belt particles during May 1998, *EOS Trans. Am. Geophys. Union, 79*, F740, 1998.

Burlaga, L., R. Fitzenreiter, R. Lepping, K. Ogilvie, A. Szabo, A. Lazarus, J. Steinberg, G. Gloeckler, R. Howard, D. Michels, C. Farrugia, R. P. Lin, and D. E. Larson, A magnetic cloud containing prominence material: January, 1997, *J. Geophys. Res., 103*, 277, 1998.

Cummings, W. D., R. J. O'Sullivan and P. J. Coleman, Standing Alfven waves in the magnetosphere, *J. Geophys. Res., 74*, 778, 1969.

Elkington, S. R., M. K. Hudson and A. A. Chan, Acceleration of relativistic electrons via drift-resonant interaction with toroidal-mode Pc-5 ULF oscillations, *Geophys. Res. Lett.,26*, 3273, 1999.

Elkington, S.R., Simulating electron radiation belt dynamics, PhD thesis, Dartmouth College, 2000.

Falthammar, C.-G., Radial diffusion by violation of the third adiabatic invariant, in *Earth's Particles and Fields*, ed. by B.M McCormac, p. 157, NATO Advanced Study Institute, Reinhold Book Corp., New York, 1968.

Goodrich, C. C., M. W. Wiltberger, R. E. Lopez, K. Papadopoulos and J. G. Lyon, An overview of the impact of the January 10 - 11, 1997 magnetic cloud on the magnetosphere via global MHD simulation, *Geophys. Res. Lett., 25*, 2537, 1998.

Hudson, M. K., A. D. Kotelnikov, X. Li, I. Roth, M. Temerin, J. Wygant, J. B. Blake, and M. S. Gussenhoven, Simulation of proton radiation belt formation during the March 24, 1991, SSC, *Geophys. Res. Lett., 22,* 291, 1995.

Hudson, M. K., S. R. Elkington, J. G. Lyon, V. A. Marchenko, I. Roth, M. Temerin and M. S. Gussenhoven, MHD/particle simulations of radiation belt formation during a storm sudden commencement, in *Radiation Belts: Models and Standards, edited by J. F. Lemaire, D. Heynderickx, and D. N. Baker, Geophys. Momogr. Ser., vol. 97, p. 57,* AGU, Washington, D. C., 1996.

Hudson, M. K., S. R. Elkington, J. G. Lyon, C. C. Goodrich and T. J. Rosenberg, Simulation of radiation belt dynamics driven by solar wind variations, *Sun-Earth*

Plasma Connections, Geophysical Monograph 109, J. L. Burch, R. L. Carovillano and S. K. Antiochos, eds., American Geophysical Union, Washington D.C., 1999.

Hudson, M. K., S. R. Elkington, J. G. Lyon and C. C. Goodrich, Increase in relativistic electron flux in the inner magnetosphere: ULF wave mode structure, *Adv. Space Res.,* 25, 2327, 2000.

Kim, H.-J. and A. A. Chan, Fully adiabatic changes in storm time relativistic electron fluxes, *J. Geophys. Res., 102*, 22107, 1997.

Li, X., I. Roth, M. Temerin, J. R. Wygant, M. K. Hudson and J. B. Blake, Simulation of the prompt energization and transport of radiation belt particles during the March 24, 1991, SSC, *Geophys. Res. Lett., 20,* 2423, 1993.

Li, X., D. N. Baker, M. Temerin, T. Cayton, G. D. Reeves, T. Araki, H. Singer, D. Larson, R. P. Lin and S. G. Kanekal, Energetic electron injections into the inner magnetosphere during the January 10-11, 1997, magnetic storm, *Geophys. Res. Lett., 25*, 2561, 1998.

Li, X., D.N. Baker, M. Temerin, T.E. Cayton, G.D. Reeves, R.S. Selesnick, J.B. Blake, G. Lu, S.G. Kanekal and H.J. Singer, Rapid enhancement of the relativistic electrons deep in the magnetosphere during the May 15, 1997, magnetic storm, *J. Geophys. Res., 104*, 4467, 1999.

Moorer, D.F. and D.N. Baker, Quantitative mapping and forecasting of high energy electron flux in the outer radiation belt, *EOS Trans. Am. Geophys. Union, 80*, 845, 1999.

Paulikas, G. A., and J B. Blake, Effects of the solar wind on magnetospheric dynamics: Energetic electrons at the synchronous orbit, *Quantitative Modeling of Magnetospheric Processes, 21*, Geophys. Monograph Series, 1979.

Rostoker, G., S. Skone and D. N. Baker, On the origin of relativistic electrons in the magnetosphere associated with some goemagnetic storms, *Geophys. Res. Lett., 25*, 3701, 1998.

Reeves, G. D., R. H. W. Friedel, R. D. Belian, M. M. Meier, M. G. Henderson, T. Onsager, H. J. Singer, D. N. Baker and X. Li, The relativistic electron response at geosynchronous orbit during the January 10, 1997, magnetic storm, *J. Geophys. Res., 103* 17559, 1998a.

Reeves, G. D., D. N. Baker, R. D. Belian, J. B. Blake, T. E. Cayton, J. F. Fennell, R. H. W. Friedel, M. M. Meier, R. S. Selesnick and H. E. Spence, The global response of relativistic radiation belt electrons to the January 1997 magnetic cloud, *Geophys. Res. Lett., 25,* 3265, 1998b.

Selesnick, R. S. and J. B. Blake, Dynamics of the outer radiation belt, *Geophys. Res. Lett., 24,* 1347, 1997.

Selesnick, R.S. and J. B. Blake, On the source location of radiation belt relativistic electrons, *J. Geophys. Res., 105*, 2607, 2000.

Shea, M. A. and D. F. Smart, March 1991 solar terrestrial phenomena and related technological consequences, in Proc. Int. Conf. Cosmic Rays, 23rd, 1993.

Southwood, D. J., Some features of field line resonances in the magnetosphere, *Planet. Space Sci., 36*, 503, 1974.

Vette, J. I., The AE8 trapped electron model environment, NSSDC/WDC-A-R&S 91-24, 1991.

Wygant, J. R., F. Mozer, M. Temerin, J. B. Blake, N. Maynard, H. Singer and M. Smiddy, Large amplitude electric and magnetic field signatures in the inner magnetosphere during injection of 15 MeV electron drift echoes, *Geophys. Res. Lett., 21*, 1739, 1994.

M. K. Hudson, S. R. Elkington, J. G. Lyon and M. Wiltberger, Physics and Astronomy Dept., Dartmouth College, Hanover, NH 03755. (email: mary.hudson@dartmouth.edu)

M. Lessard, Thayer School of Engineering, Dartmouth College, Hanover, NH 03755

Received ______________________

This manuscript was prepared with AGU's LaTeX macros v4, with the extension package 'AGU^{++}' by P. W. Daly, version 1.5d from 1997/04/28.

Figure Captions

Figure 1. Simulated equatorial plane flux vs. energy and L for four geomagnetic storm events. Time intervals shown are from (a)27 August 1998, 0430-1330 UT, (b)4 May 1998, 0300-1000 UT, (c)15 May 1997, 0000-1230 UT, and (d)10 January 1997, 0200-1630 UT, starting with AE8MIN source population, advanced in time using equatorial plane fields from 3D MHD simulation driven by WIND input. Frame spacing is $\sim$ (a) 1.5 hours for total of 9 hrs; (b) 1.5 hours for total of 7.5 hrs; (c) 2:05 hrs for total of 12.5 hrs; and (d) 3.625 hours for total of 14.5 hrs.

Figure 2. Simulated equatorial plane differential flux vs. energy and L for 4 May 1998, 0300-1000 UT, at 1.5 hour intervals for a total of 7.5 hrs. Electron source population from HEO spacecraft measurements on 1 May 1998 (J. F. Fennell, private communication).

Figure 3. (a)Power spectrum of simulated radial electric field component at midnight $\pm$ 1 hour LT for 7.5 to 10.5 UT on 26 Aug 1998; (b)same for 4.5 to 7.5 UT on 27 Aug 1998. Ascending black lines indicate dipole drift frequency as a function of L for electrons with energies indicated; descending lines show same for constant first invariant, same energies. Note power spectral density scale is doubled in (b) relative to (a).

Figure 4. GOES 8 magnetic field data for 26-27 August 1998, plotted from 1 minute averaged key parameter data in a mean field coordinate system, radial (top), east or azimuthal (middle) and north or compressional components; FFT spectra are shown above each time series.

Figures

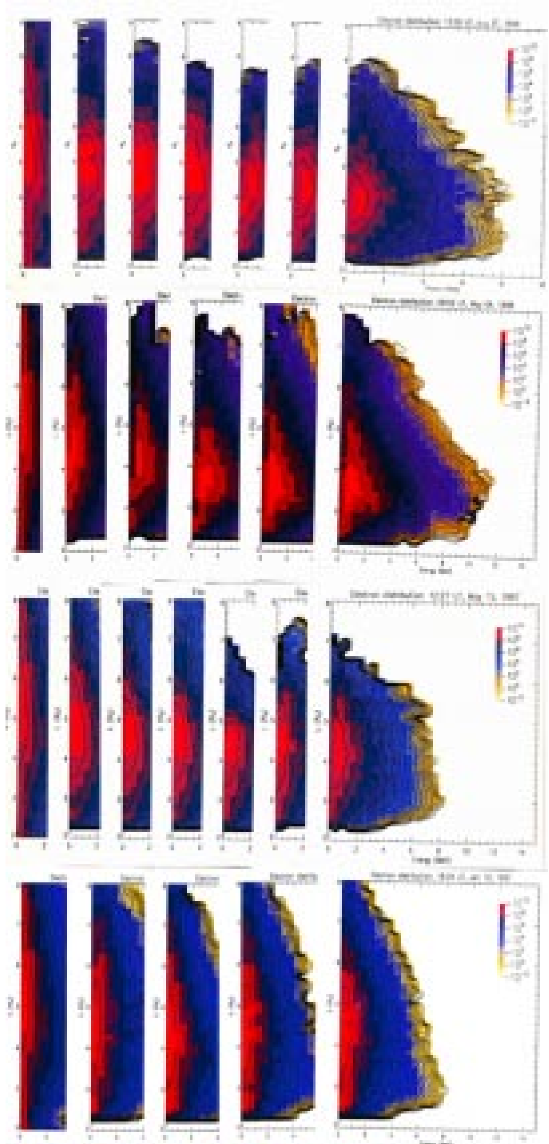

Figure 1. Simulated equatorial plane flux vs. energy and L for four geomagnetic storm events. Time intervals shown are from (a)27 August 1998, 0430-1330 UT, (b)4 May 1998, 0300-1000 UT, (c)15 May 1997, 0000-1230 UT, and (d)10 January 1997, 0200-1630 UT, starting with AE8MIN source population, advanced in time using equatorial plane fields from 3D MHD simulation driven by WIND input. Frame spacing is $\sim$ (a) 1.5 hours for total of 9 hrs; (b) 1.5 hours for total of 7.5 hrs; (c) 2:05 hrs for total of 12.5 hrs; and (d) 3.625 hours for total of 14.5 hrs.

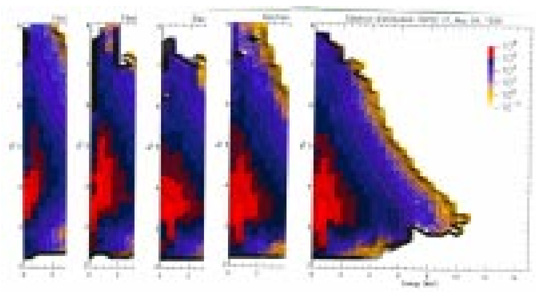

Figure 2. Simulated equatorial plane differential flux vs. energy and L for 4 May 1998, 0300-1000 UT, at 1.5 hour intervals for a total of 7.5 hrs. Electron source population from HEO spacecraft measurements on 1 May 1998 (J. F. Fennell, private communication).

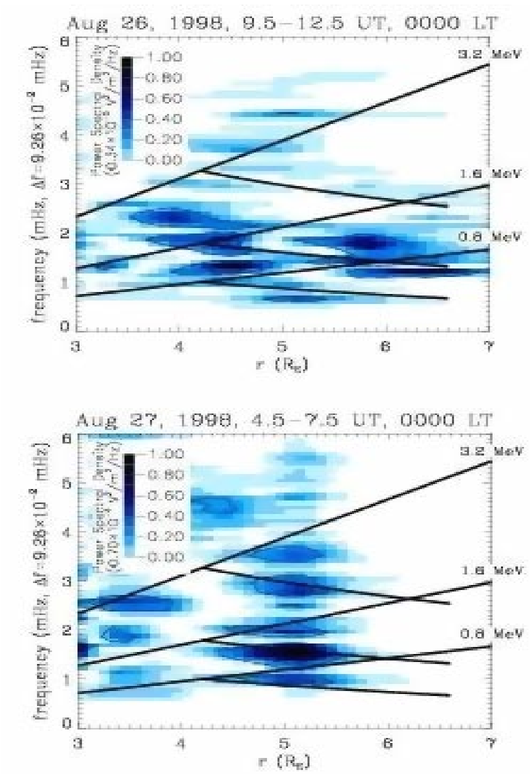

Figure 3. (a)Power spectrum of simulated radial electric field component at midnight $\pm$ 1 hour LT for 7.5 to 10.5 UT on 26 Aug 1998; (b)same for 4.5 to 7.5 UT on 27 Aug 1998. Ascending black lines indicate dipole drift frequency as a function of L for electrons with energies indicated; descending lines show same for constant first invariant, same energies. Note power spectral density scale is doubled in (b) relative to (a).

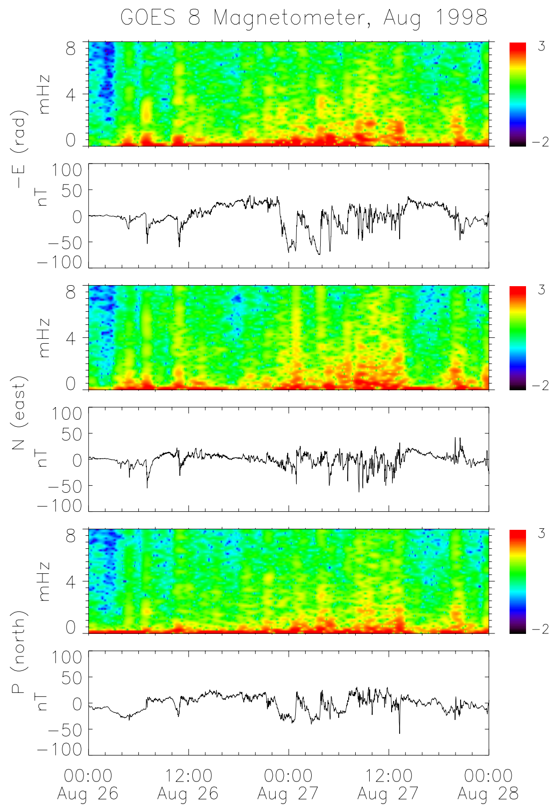

Figure 4. GOES 8 magnetic field data for 26-27 August 1998, plotted from 1 minute averaged key parameter data in a mean field coordinate system, radial (top), east or azimuthal (middle) and north or compressional components; FFT spectra are shown above each time series.